Elasticity control of entangled chromosomes: crosstalk between condensin complexes and nucleosomes

Tetsuya Yamamoto[1], Kazuhisa Kinoshita[2], and Tatsuya Hirano[2]

[1]Institute for Chemical Reaction Design and Discovery (ICReDD), Hokkaido University, Sapporo, Hokkaido 001-0021, Japan.
[2]Chromosome Dynamics Laboratory, RIKEN, Wako, Saitama, Japan.

E-mail: tyamamoto@icredd.hokudai.ac.jp

Condensin-mediated loop extrusion is now considered the main driving force of mitotic chromosome assembly. Recent experiments have shown, however, that a class of mutant condensin complexes deficient in loop extrusion can assemble abnormal chromosome-like structures in *Xenopus* egg extracts. In the absence of topoisomerase II (topo II), the mutant condensin complexes produce an unusual round-shaped structure termed a `bean', which is composed of a DNA-dense central core surrounded by a DNA-sparse halo. The mutant condensin complexes accumulate in the core whereas histones are more concentrated in the halo than in the core. To get insights into how the bean structure is formed, here we construct a theoretical model. Our theory predicts that the core is produced by the attractive interactions between mutant condensin complexes whereas the halo is stabilized by the energy reduction by the selective accumulation of nucleosomes. The formation of the halo increases the elastic free energy due to the DNA entanglement in the core, but the latter free energy is compensated by condensin complexes that protect DNAs from nucleosome assembly. Understanding this peculiar structure is likely to enrich our understanding of how DNA entanglements, nucleosomes, and condensin functionally cross-talk with each other.

INTRODUCTION

At the entry into mitosis, chromosomal DNAs exhibit a series of dramatic structural transitions from the relatively diffuse interphase chromatin structures to a discrete set of rod-shaped structures, each composed of duplicated sister chromatids. This process, collectively referred to as mitotic chromosome assembly, is essential for the faithful segregation of genetic information into daughter cells. Extensive studies during the past two decades or so have fully established that condensins, a class of SMC protein complexes, play a central role in this process (Hirano, 2016). Although it remains unknown exactly how condensins might work at a mechanistic level, the so-called loop extrusion theory has attracted much attention recently (Alipour and Marko, 2012, Naumova et al., 2013, Goloborodko et al., 2016a and

2016b). The theory originally predicted that the rod-shaped structure of mitotic chromosomes is assembled by the loop extrusion mechanism. Subsequent demonstration that budding yeast condensin has the activity to translocate along a DNA (Terakawa et al., 2017) and to extrude DNA loops (Ganji et al., 2018, Kong et al., 2020) in vitro has provided strong experimental support for this theory.

Is the mechanism of loop extrusion mediated by condensins sufficient to assemble mitotic chromosomes? Early studies demonstrated that *Xenopus laevis* condensin I has the activity to introduce positive superhelical torsion into double-stranded DNAs (Kimura and Hirano, 1997). Moreover, it is not fully understood how condensins extrude chromatinized DNA substrates or how they functionally cross-talk to other chromosomal components, such as topoisomerase II (topo II) and histones, during mitotic chromosome assembly (Shintomi et al., 2015; Shintomi et al., 2017, Choppakatia et al., 2021; Shintomi et al., 2021). Experiments using *Xenopus* egg extracts have shown that mutant condensin complexes deficient in loop extrusion are not completely defective in chromosome assembly (Kinoshita et al. 2015; Kinoshita et. al., 2022; see Fig. 1**a**). Notably, under the condition where DNA entanglements between different chromosomes persist in the absence of topo II, the addition of the mutant condensin complexes converts a swollen DNA network (Fig. 1**b**) into an unusually compact structure, called a `bean', that is composed of a DNA-dense core and a DNA-sparse halo (Fig. 1**c**). The mutant condensin complexes accumulate in the core whereas histones are more concentrated in the halo than in the core. These studies raised the possibility that a loop extrusion-independent mechanism contributes to mitotic chromosome assembly and shaping. It has been proposed that condensin-condensin interactions through its HEAT repeat subunit could underlie these processes (Sakai et al. 2018; Kinoshita et al. 2022). Another example of a loop extrusion-independent mechanism of DNA compaction by SMC protein complexes has been suggested through experiments using a mixture of bare DNAs and yeast cohesin complexes (Ryu et al., 2021). In this study, DNA condensation was explained by DNA-cohesin-DNA bridging.

Entanglements restrict the fluctuation of polymer chains and are treated as effective crosslinks in polymer physics (Edwards, 1967, Rubinstein and Colby, 2003). Unlike chemical crosslinks, these effective crosslinks can slide along the chains and are therefore called slip-links (Ball et al., 1981, Masubuchi, 2021) or slip-springs (Likhtman, 2005, Uneyama and Masubuchi, 2012). In the absence of topo II, entanglements between different chromosomes are not dissolved in the experimental time scale (Rosa and Everaers, 2008) and thus can be treated as an entangled polymer network (Fig. 1**c**). In general, when the polymer network is stretched, a subset of chains in the network is stretched and contributes to the elasticity of

the network (elastically effective chains; the black broken lines in Fig. 2**a**) (Rubinstein and Colby, 2003). The other chains such as dangling loops, which do not respond to the stretching of the network, do not contribute to the elasticity of the network (elastically ineffective chains). When nucleosomes are assembled, DNA sections wrapped around histones become elastically ineffective (the cyan broken lines in Fig. 2**b**). We also count the DNA loops in the halo of a bean elastically ineffective because these loops are treated separately from the network in the core (Fig. 2**c**). Polymer physics predicts that the stiffness of each elastically effective chain increases with decreasing the number of DNA units in the chain (Rubinstein and Colby, 2003). The formation of nucleosomal loops in the halo stiffens the entangled DNA network because they reel DNAs out of the core and decrease the number of DNA units in the elastically effective part of entangled DNA in the core. Recently, a similar concept was used to theoretically predict the contribution of the loop extrusion process to the self-assembly of entangled bare DNAs (Yamamoto and Schiessel, 2022). The electrostatic aspect of the nucleosome assembly, such as the charge inversion (Park et al., 1999, Nguyen and Shklovskii, 2001), is a classical subject of soft matter physics. However, the regulation of DNA elasticity by functional crosstalk between nucleosomes and condensin complexes is only rarely studied, especially in the context of large-scale chromosome assembly.

To provide insight into the loop extrusion-independent mechanism of chromosome assembly, we here construct a minimal theory of the behavior of entangled DNAs under the condition where mutant condensin complexes deficient in loop extrusion form beans in *Xenopus* egg extracts. In the spirit of classical theoretical physics, we make the theory as simple and general as possible, instead of taking into account the fine details of a specific system. Our theory predicts that the mutant condensin complexes drive the formation of the DNA-dense and nucleosome-poor central core of a bean whereas the DNA-sparse halo is stabilized by the energy reduction by the selective accumulation of nucleosomes. The formation of the halo in turn increases the free energy contribution of the DNA entanglement in the core and also increases the free energy contribution of the excluded volume interaction between nucleosomal DNAs in the halo. The mutant condensin complexes compensate the entanglement free energy by protecting DNAs from nucleosome assembly and entrap the bean structure in the local free energy minimum. The free energy contribution of the excluded volume interaction of nucleosomal DNAs in the halo remains and thus the bean structure is not the global free energy minimum. This implies that the bean structure is assembled by a kinetic trap or there is a mechanism that further stabilizes this structure.

MATERIALS AND METHODS

Mechanical properties of bare and nucleosomal DNA

In an aqueous solution of physiological concentration, the electric charges of DNAs are neutralized by the Manning condensation and the Debye-Huckel screening due to salt ions (Marko and Siggia, 1995, Bracha et al., 2013). The unit length b_0 of a bare DNA is 100 nm ($\approx$ 300 bps) (Marko and Siggia, 1995). In a recent experiment on yeast, the unit length b of nucleosomal DNAs was estimated as 50 nm and there are 2 nucleosomes per 10 nm (Socol et al., 2019). A stretch of DNA is wound around an octamer of histone proteins by $\approx$146 bps in each nucleosome and nucleosomes are spaced by linker DNA regions of $\approx$ 19 bps: DNA of length 1.65 kbps is thus included in a Kuhn length of nucleosomal DNA. In this paper, we define a DNA unit as the DNA in a Kuhn length of bare DNA. g_{n} ($\approx$ 5.5) is the ratio of DNA in a Kuhn length of nucleosomal DNA to that of a DNA unit. Chromosomes are much longer than either of the two Kuhn lengths, b_0 and b, and are treated as electrically neutral flexible polymers.

Model of the bean structure

In this theory, we treat entangled chromosomes composed of N DNA units in an aqueous solution, including histone and the mutant condensin complexes deficient in loop extrusion (Fig. 3). For simplicity, we treat these chromosomes as homogeneous polymers. The bean structure is composed of the core and the halo. We treat the core as a network of entangled DNAs and the halo as DNA loops packed at the surface of the core. A fraction N_{c}/N of DNA units are distributed to the core, while the other units are distributed to the halo. The second law of thermodynamics states that the most stable state is given by the minimum of the free energy. In this theory, we seek the mechanism of the assembly of the bean structure by analyzing the state of the minimum free energy.

The free energy F of the system is represented as the sum of the free energy F_{c} of the core and the free energy F_{h} of the halo,

$$F = F_{\mathrm{c}} + F_{\mathrm{h}}. \tag{1}$$

For simplicity, we use the mean field theory, an extension of the Flory-Rehner theory (Flory and Rehner, 1943) for the core and an extension of the Alexander theory (Alexander, 1977, de Gennes, 1980) for the halo, to derive the free energy of the core and the halo, and we limit our discussion to a spherical bean.

The free energy of the core has the form

$$F_{\mathrm{c}} = (f_{\mathrm{ent}} + f_{\mathrm{sol}} + f_{\mathrm{bnd}})\, V_{\mathrm{c}}, \tag{2}$$

where V_{c} is the volume of the core. f_{ent} is the elastic free energy of DNAs in the core due to the entanglement. f_{sol} is the solution free energy, including the free energy contributions of the mixing entropy and the interactions between the mutant condensin complexes. f_{bnd} is the binding free energy, including the contributions of the assembly of nucleosomes and the loading of the mutant condensin complexes. The structure of the core is quantified by the volume fraction ϕ of DNAs, the occupancies of DNA units by nucleosomes α_{h} and the mutant condensin complexes α_{c}.

The free energy of the halo has the form

$$F_h = \int_{r_{\mathrm{c}}}^{r_{\mathrm{b}}} dr\, 4\pi r^2\, f_{\mathrm{h}}, \tag{3}$$

where r is the radial coordinate to represent positions in a bean structure by the distance from the center of the spherical bean. r_{c} is the radius of the core and r_{b} is the radius of the bean. The free energy density of the halo has three contributions

$$f_{\mathrm{h}} = f_{\mathrm{lop}} + f_{\mathrm{sol}} + f_{\mathrm{bnd}}, \tag{4}$$

where, f_{lop} is the elastic free energy of DNA loops in the halo. The elastic free energy f_{lop} is independent of the entanglement and is different from f_{ent} in eq. (2). f_{sol} is the solution free energy and f_{bnd} is the binding free energy. The free energy contributions, f_{sol} and f_{bnd}, are the same as the second and third terms in the integrand of eq. (2). These free energy densities are functions of the local DNA volume fraction ϕ, the local occupancies of nucleosomes α_{h} and the mutant condensin complexes α_{c}, which are functions of the coordinate r.

The volume V_{c} and radius r_{c} of the core has a relationship with the volume fraction ϕ of DNAs,

$$V_{\mathrm{c}} = \frac{4\pi}{3} r_{\mathrm{c}}^3 = \frac{b^3 N_{\mathrm{c}}}{\phi}. \tag{5}$$

The radius r_{b} of the bean also has a relationship with the DNA volume fraction

$$\int_{r_{\mathrm{c}}}^{r_{\mathrm{b}}} dr\, 4\pi r^2 \phi = b^2 (N - N_{\mathrm{c}}). \tag{6}$$

Elastic free energy due to the entanglement

In polymer physics, the entanglement is treated as effective crosslinks. These effective crosslinks are distributed uniformly in the core, while there are no entanglements in the halo. We use the simplest model of polymer entanglement, the affine tube model, that predicts that the effective crosslinks due to the entanglement are fixed at the space (more precisely, this theory takes into account the Gaussian fluctuation around the fixed point, but it does not change the physics) (Edwards, 1967, Rubinstein and Colby, 2003). In contrast to chemical crosslinks, chains can slide through the effective crosslinks. If we assume the DNAs are nucleosomal in the relaxed state (which is called the reference state), the end-to-end distance of a DNA chain is

$$R_0 = b\left(\frac{N_{\mathrm{e0}}}{g_{\mathrm{n}}}\right)^{\frac{1}{2}}, \tag{7}$$

where N_{e0} is the number of units in a DNA between two effective crosslinks in the relaxed state (count by bare DNA units). When the DNA network is swollen or deswollen so that the dimension of the network changes by λ_{s} times (λ_{s} is called the swelling ratio), the positions of effective crosslinks displace with the same ratio (the affine deformation), see Fig. 4. The end-to-end distance of the DNA chain thus changes to $\lambda_s R_0$.

In the reference state, all DNA units are distributed to the core. In the bean structure, some DNA units are distributed to the halo and thus the number of DNA units in the core decrease from that of the reference state. DNA units are distributed to make the tensions of chains between effective crosslinks equal. Because the number of effective crosslinks is constant, the number N_{e} of DNA units between two effective crosslinks in the bean structure has the form

$$\frac{N_{\mathrm{e}}}{N_{\mathrm{e0}}} = \frac{N_{\mathrm{c}}}{N}, \tag{8}$$

where N_{c} is the total number of DNA units in the core and N is the total number of DNA units in the system. If the DNA chain is bare, the square δR^2 of the amplitude of the fluctuations of the chain is $b_0^2 N_{\mathrm{e}}$, whereas, if the DNA chain is fully packed with nucleosomes, δR^2 is $b^2 N_{\mathrm{e}}/g_{\mathrm{n}}$. We use the linear approximation

$$\delta R^2 = b^2 \frac{N_{\mathrm{e}}}{g_{\mathrm{n}}} \alpha_{\mathrm{h}} + b_0^2\, N_{\mathrm{e}}(1 - \alpha_h) \tag{9}$$

to treat cases in which the occupancy of DNA units by nucleosomes is α_{h}. We take into

account the fact that DNA units wound around histone proteins and those at the halo are elastically ineffective via eq. (9). The linear approximation corresponds to the serial connection of a spring of bare DNA and a spring of nucleosomal DNA and is exact if we only take into account the changes in the number of DNA units in the elastically effective part of the chain, $b \to b_0$ and $g_\mathrm{n} \to$ 165 bps/19 pbs $\approx$ 8.7. In the treatment of eq. (9), we also take into account the difference in the unit length between nucleosomal DNAs and bare DNAs up to the linear term of α_h.

The volume fraction of DNA units is ϕ_0 in the reference state. This volume fraction does not include the volume of histone and thus is independent of the state of DNAs. In the core of the bean, the volume fraction of DNA units changes to

$$\phi = \frac{\phi_0}{\lambda_\mathrm{s}^3}\frac{N_\mathrm{e}}{N_\mathrm{e0}} \tag{10}$$

because the volume of the core changes by λ_s^3 by the swelling or deswelling and the number of DNA units in the core decreases to N_e because of the assembly of halo.

The elastic free energy density is the elastic energy of each chain $\frac{3}{2}k_B T\frac{\lambda_s^2 R_0^2}{\delta R^2}$, multiplied by the volume density $\phi/(b^3 N_\mathrm{e})$ of DNA in the network (Rubinstein and Colby, 2003, Yamamoto et al., 2022),

$$f_\mathrm{ent} = \frac{3}{2}\frac{\phi}{b^3 N_\mathrm{e}} k_\mathrm{B} T \frac{\lambda_\mathrm{s}^2 R_0^2}{\delta R^2}. \tag{11}$$

Eq. (11) is simplified to

$$f_\mathrm{ent} = \frac{3}{2}\frac{G_0}{\lambda_\mathrm{s}}\frac{N_\mathrm{e0}}{N_\mathrm{e}}\frac{1}{\alpha_\mathrm{h} + \rho(1-\alpha_\mathrm{h})} \tag{12}$$

by using eq. (10) and the shear modulus of the network at the reference state

$$G_0 = k_B T \frac{\phi_0}{b^3 N_\mathrm{e0}}. \tag{13}$$

The factor ρ is the ratio of the squared amplitudes of fluctuations between the bare and nucleosomal DNA with the same DNA length,

$$\rho = \frac{b_0^2 g_\mathrm{n}}{b^2}. \tag{14}$$

The factor $N_{\mathrm{e0}}/N_{\mathrm{e}}$ in eq. (12) represents the stiffening of the entangled DNAs in the core due to DNAs reeled out from the core to the halo. The factor $1/(\alpha_{\mathrm{h}}+\rho(1-\alpha_{\mathrm{h}}))$ in eq. (12) represents the stiffening of the entangled DNAs in the core due to the nucleosomal assembly at the entangled DNAs in the core.

Solution free energy

The solution free energy includes the contribution of the mixing entropy and the contribution of the condensin-condensin interactions. The conformational transitions of condensin complexes influence the interactions between these complexes (Kinoshita et al., 2015). The key feature of the conformational transitions, revealed by recent X-ray (Hassler et al., 2019) and cryo-EM (Lee et al., 2020), is that the SMC4 subunit binds to SMC2 in the presence of ATP whereas it binds to CAP-D2 in the absence of ATP (a flip-flop mechanism). It has been proposed that a condensin-condensin interaction is triggered by a contact between SMC4 in one complex with CAP-D2 in another complex in the absence of ATP (Kinoshita et al., 2022).

The kinetics of the fraction θ of the mutant condensin complexes, to which ATPs are not bound and thus interact with other condensin complexes, is represented by the time evolution equation

$$\frac{d}{dt}\theta = k_{\mathrm{on}}\theta - k_{\mathrm{off}}(1-\theta). \tag{15}$$

In the steady state, the fraction θ is derived as

$$\theta = \frac{1}{1+\frac{k_{\mathrm{off}}}{k_{\mathrm{on}}}} \tag{16}$$

by using eq. (15). The free energy density due to the interaction between condensin complexes has the form

$$f_{\mathrm{int}} = -\frac{k_{\mathrm{B}}T}{b_0^3}\chi\alpha_{\mathrm{c}}^2\phi(1-\phi), \tag{17}$$

where χ is the magnitude of the interaction between the mutant condensin complexes. The interaction parameter χ has the form

$$\chi = \chi_0\theta^2 \tag{18}$$

because ATPs are not bound to both of the two interacting condensin complexes.

The solution free energy density has the form

$$f_{\mathrm{sol}} = \frac{k_{\mathrm{B}}T}{b_0^3}[(1-\phi-\alpha_{\mathrm{h}}\phi-\alpha_{\mathrm{c}}\phi)\log(1-\phi-\alpha_{\mathrm{h}}\phi-\alpha_{\mathrm{c}}\phi)-\chi\alpha_{\mathrm{c}}^2\phi(1-\phi)], \qquad (19)$$

where the first term in the square bracket is the free energy contribution of the mixing entropy (the mixing free energy). The mixing free energy quantifies the random thermal motion that mixes DNA units and solvent and acts as the effective excluded volume interaction between DNA units (Rubinstein and Colby, 2003). The swelling of polymer networks is driven by this effective excluded volume interaction. The factor $\alpha_{\mathrm{h}}\phi$ represents the increase of the excluded volume due to the assembly of nucleosomes and the factor $\alpha_{\mathrm{c}}\phi$ is the increase of excluded volume due to the loading of condensin complexes. For simplicity, we assume that for both cases, the increase of the excluded volume is the same as the volume of DNA units. The free energy contribution of the excluded volume interaction is included in the first term of eq. (19).

Binding free energy

The binding free energy has the form

$$f_{\mathrm{bnd}} = \frac{k_{\mathrm{B}}T}{b_0^3}\phi[\alpha_{\mathrm{h}}\log\alpha_{\mathrm{h}}+\alpha_{\mathrm{c}}\log\alpha_{\mathrm{c}}+(1-\alpha_{\mathrm{h}}-\alpha_{\mathrm{c}})\log(1-\alpha_{\mathrm{h}}-\alpha_{\mathrm{c}})+(\epsilon_{\mathrm{h}}-\mu_h)\alpha_{\mathrm{h}}+(\epsilon_{\mathrm{c}}-\mu_c)\alpha_{\mathrm{c}}]. \quad (20)$$

The first, second, and third terms are the free energy contributions of the entropy with respect to the assembly of nucleosomes and the loading of the mutant condensin complexes. With this treatment, we assume that nucleosomes and the mutant condensin complexes cannot occupy the same DNA site simultaneously, $\alpha_{\mathrm{h}}+\alpha_{\mathrm{c}} \leq 1$. The chemical potentials, μ_{h} $(=\log\phi_{\mathrm{h}}^{\mathrm{ex}})$ and μ_{c} $(=\log\phi_{\mathrm{c}}^{\mathrm{ex}})$, are the logarithms of the volume fractions, $\phi_{\mathrm{h}}^{\mathrm{ex}}$ and $\phi_{\mathrm{c}}^{\mathrm{ex}}$, of histones and the mutant condensin complexes in the solution at the exterior to the bean. The fourth term is the energy gain $k_{\mathrm{B}}T\epsilon_{\mathrm{h}}$ due to the assembly of a nucleosome, relative to the chemical potential $k_{\mathrm{B}}T\mu_{\mathrm{h}}$ of histone proteins. The fifth term results from the stabilizing energy $k_{\mathrm{B}}T\epsilon_{\mathrm{c}}$ due to the loading of the mutant condensin complexes, relative to the chemical potential $k_{\mathrm{B}}T\mu_{\mathrm{c}}$ of these mutants. In our theory, we assume that the mutant condensin complexes bound to DNA are distributed uniformly in the core and do not have to explicitly take into account the thermal diffusion of the mutants along DNA.

Elastic free energy of DNA loops

The DNA loops in the halo are packed and stretched. These loops are analogous to a polymer brush, which is prepared by end-grafting polymers to a surface. The simplest treatment of a polymer brush is the Alexander model which assumes that the concentration of polymer units is uniform in the brush for the limit of vanishing curvature (Alexander, 1977, de Gennes, 1980).

The DNA loops can be divided into `blobs' composed of g DNA units, which occupy the volume ξ^3, where ξ is the average distance between DNA chains at the same distance r from the center (de Gennes, 1980). The effect of the curvature on the elastic free energy is taken into account in the spirit of the Daoud-Cotton scaling theory (Daoud and Cotton, 1982). Because the spherical surface at a distance r is occupied by the blobs, the average distance ξ has a relationship

$$4\pi r^2 = 2n\xi^2, \tag{21}$$

where n is the number of DNA loops and 2 in front of n represents the fact that each DNA loop contributes two DNA chains to the area (in this paper, we treat n as a constant, for simplicity). The elastic energy of the DNA loops in the halo thus has the form

$$\int_{r_\mathrm{c}}^{r_\mathrm{b}} 4\pi r^2 f_\mathrm{lop} = \int_{r_\mathrm{c}}^{r_\mathrm{b}} \frac{4\pi r^2 dr}{\xi^3} \frac{3}{2} k_\mathrm{B} T \frac{\xi^2}{\delta R(g)^2}, \tag{22}$$

because the elastic free energy of each blob is $\frac{3}{2} k_\mathrm{B} T \frac{\xi^2}{\delta R(g)^2}$ and $\frac{4\pi r^2 dr}{\xi^3}$ is the number of blobs at the distance r, where $\delta R(g)$ is eq. (9), but N_e is replaced with g. The volume fraction of DNA units in the halo has the form

$$\phi(r) = \frac{b^3 g}{\xi^3}. \tag{23}$$

By using eqs. (21) and (23), eq. (22) is rewritten as a functional of $\phi(r)$ and r. This leads to the elastic free energy density of the loops in the form

$$f_\mathrm{lop} = \frac{3}{2} \frac{1}{\phi} \frac{r_\mathrm{m}^4}{r^4} \frac{1}{b_0^3} \frac{\rho}{\alpha_\mathrm{h} + \rho(1 - \alpha_\mathrm{h})} \tag{24}$$

with

$$r_\mathrm{m}^2 = \frac{nb^2}{4\pi}. \tag{25}$$

In the scaling theory of polymer brushes, the relationship between ξ and g is derived by the Flory theory, which corresponds to using eq. (44) (or just assumed that the relationship is given *a priori*), and the free energy used for other purposes is estimated by $k_\mathrm{B}T$ per blob (de Gennes, 1980). For simplicity, we here use eq. (44) for all purposes, although the scaling theory is quantitatively a better approximation.

Parameter estimate

Our theory predicts the DNA volume fraction ϕ, the occupancies, α_{h} and α_{c}, of nucleosomes and the mutant condensin complexes, and the fraction N_{c}/N of DNA in the core as functions of the rescaled shear modulus $G_0 b_0^3/(\phi_0^{\frac{1}{3}} k_{\mathrm{B}} T)$, the free energy $\epsilon_{\mathrm{h}} - \mu_{\mathrm{h}}$ gained by assembling nucleosomes, the free energy $\epsilon_{\mathrm{c}} - \mu_c$ gained by loading the mutant condensin complexes, the interaction parameter χ, the ratio ρ of the size of bare DNAs to nucleosomal DNAs (see eq. (14)), and the volume ratio ϕ_{m} defined by

$$\phi_{\mathrm{m}} = \frac{N b_0^3}{\frac{4\pi r_{\mathrm{m}}^3}{3}}, \tag{26}$$

where r_{m} is the radius of a sphere with which the surface area is packed with DNA units of n DNA loops, see eq. (25). Eq. (26) can be considered as the ratio of the total volume $N b_0^3$ of DNA to the volume $4\pi r_{\mathrm{m}}^3/3$ of DNA in the core for a `DNA elastomer', with which the entangled DNA network is deswollen by eliminating all the solvent molecules, histone proteins, and the mutant condensin complexes. The values of the parameters used for the numerical calculation are listed in Table 1.

Symbol	Physical meaning	Estimate	Used value
$G_0 b_0^3/(\phi_0^{\frac{1}{3}} k_{\mathrm{B}} T)$	Dimensionless shear modulus	Not available	0.01
$\epsilon_{\mathrm{h}} - \mu_{\mathrm{h}}$	Dimensionless energy to assemble nucleosomes	-3	-2
$\epsilon_{\mathrm{c}} - \mu_c$	Dimensionless energy to load the mutant condensin complexes	Not available	Varied
χ	Interaction parameter	Not available	9
ρ	Ratio of bare and nucleosomal DNA size	22	22
ϕ_{m}	Ratio of total DNA to DNA at core	8.7	8

Table 1 Values of parameters used for numerical calculations

Naively, the volume ratio is estimated as $\phi_{\mathrm{m}} \approx$ 165 bps/19 bps $\approx$ 8.7 by assuming that

DNA units that remain without assembling nucleosomes in the core become the halo of the DNA elastomer. The ratio ρ is estimated as 8.7 if we only take into account the changes in the number of DNA units in the elastically effective part of the network by assembling nucleosomes and as 22 for cases in which we also take into account the changes of Kuhn length by the assembly. The chemical potential of histone proteins is estimated as -12 by using the histone concentration 7 μM in the *Xenopus* egg extract and a rough estimate of the volume of histone proteins 1 nm^3. This estimate assumes that histone octamers are assembled prior to the assembly of nucleosomes. The energy gained by assembling nucleosomes is estimated as -15 (Blossey and Schiessel, 2011). In principle, the rescaled shear modulus $G_0 b_0^3/(\phi_0^{\frac{1}{3}} k_{\mathrm{B}} T)$ can be extracted by measuring the force-extension relationship of the entangled chromosome though it has not been characterized.

RESULTS

The bean structure is stabilized by the free energy gained by assembling nucleosomes

The DNA volume fraction ϕ, the occupancies, α_{h} and α_{c}, of DNA units by nucleosomes and the mutant condensin complexes, and the fraction N_{c}/N of DNA units in the core of the stable structure are derived by using the conditions that the first derivatives of the free energy F with respect to these parameters are zero (see sec. S1 in the Supplemental File for the details of the mathematics). These conditions correspond to the fact that the chemical potentials of histone and the mutant condensin complexes as well as the osmotic pressure are uniform both in the core and the halo in the steady state. The condition of uniform osmotic pressure in the halo is effective for cases in which the thickness of the halo is smaller than the radius of the core. In a window of the concentrations of the mutant condensin complexes, we found a solution with which the core of the entangled DNA network becomes condensed with DNAs and the mutant condensin complexes, while DNA loops in the halo are occupied by nucleosomes and extended because of the excluded volume interactions between nucleosomal DNA units, see Fig. 5. This solution will be called the bean state because the features of this solution are consistent with the experimentally observed bean structure. In the bean state, the energy gained by assembling nucleosomes (the fourth term of eq. (20)) is dominant in the free energy at the halo, while the free energy due to the interaction between the mutant condensin complexes (the second term of eq. (19)) and the energy gained by loading these complexes (the fifth term of eq. (20)) are dominant in the free energy at the core, see also eqs. (S38) and (S53) in the Supplemental File. The DNA looping in the halo is thus driven by the assembly of nucleosomes on the DNAs in the halo.

DNAs are reeled into the core when the concentration of mutant condensin complexes is increased

Our theory can predict the radii, r_{c} and r_{b}, of the core and the bean by using eq. (5) and (6), respectively. The radius of the core increases with increasing the concentration of the mutant condensin complexes in the solution, while the radius of the bean decreases, see Fig. 6**a**. This feature is consistent with our recent experiments (Kinoshita et al., 2022). It is because the condensed state of DNAs in the core becomes more stable as the concentration of the mutant condensin complexes increases and thus the swollen DNAs at the halo are reeled into the core to gain the free energy due to the condensin-condensin interaction, see Fig. 6**b**. The sliding capability of the entanglement enables the exchange of DNA between the core and the halo. Quantitatively, our theory does not predict the maximum separation between r_{c} and r_{b} as dramatic as the experiment (Kinoshita et al., 2022). The maximum separation is sensitive to the values of parameters, such as the volume ratio ϕ_{m}, see Figs. S1**c**-S4**c**. For the condensin concentrations larger than a threshold value $\exp(\mu_{\mathrm{c}}^{\mathrm{max}})$, the halo is no longer stable and all the DNAs are condensed into the core (all-condensed state; see Fig. 2**a**, right).

Bean is a kinetically trapped structure

The fact that the halo is stabilized by the energy gained by assembling nucleosomes implies that entangled DNAs are more stable if it is fully occupied by nucleosomes. Indeed, such a state (which will be called all-swollen state; Fig. 2**a**, left) satisfies the conditions of the free energy minimum (namely, the first derivatives of the free energy are zero). The free energy of the all-swollen state is smaller than the free energy of the bean state (for several sets of parameter values that we tried), implying that the bean state is a local free energy minimum, but not the global free energy minimum, see Fig. 7. The energy gained by loading condensin and the condensin-condensin interaction stabilizes the condensed core (see eqs. (S38) and (S53) in the Supplemental File), implying that the bean structure is entrapped to a local free energy minimum by the mutant condensin complexes. The entangled DNA network shows the bean state if one decreases the concentration of the mutant condensin complexes from the all-condensed state, but not if one increases the concentration of the mutant condensin complexes from the all-swollen state. Our theory therefore predicts that the experimentally observed bean structure was kinetically trapped or there is an additional mechanism that further stabilizes the bean structure (see also DISCUSSION).

Condensin complexes protect DNAs from nucleosomal assembly in the core and compensate the stiffening of entangled DNA network

Among parameters used in our theory, the interaction parameter χ and the rescaled shear modulus $G_0 b_0^3/(\phi_0^{\frac{1}{3}} k_\mathrm{B} T)$ have not been experimentally determined. One may think that there may be a parameter space, in which the bean structure becomes the global free energy minimum. To be the global free energy minimum, the bean structure has to be stabilized up to the concentration of the mutant condensin complexes at the transition between all-swollen and all-condensed states. The maximum chemical potential $\mu_\mathrm{c}^\mathrm{max}$ of the mutant condensin complexes, with which the bean structure is stable, and the chemical potential $\mu_\mathrm{c}^\mathrm{th}$ at the swollen-condensed transition are therefore the key quantity to discuss the stability of the bean structure (the following discussion is better presented by using the chemical potential, $\mu_c = \log \phi_\mathrm{c}^\mathrm{ex}$, than the condensin concentration $\phi_\mathrm{c}^\mathrm{ex}$ of the external solution). We therefore repeated the numerical calculations by changing the values of parameters, see Figs. S1 – S4 in the Supplemental File. The maximum chemical potential $\mu_\mathrm{c}^\mathrm{max}$ of the bean structure was sensitive to the volume ratio ϕ_m, rather than the rescaled shear modulus $G_0 b_0^3/(\phi_0^{\frac{1}{3}} k_\mathrm{B} T)$, see Figs. S1**c** and S2**c**. The maximum chemical potential $\mu_\mathrm{c}^\mathrm{max}$ depends on the interaction parameter and the energy gained by assembling nucleosomes, but the chemical potential $\mu_\mathrm{c}^\mathrm{th}$ at the transition shows similar dependence, see Fig. S3**c** and S4**c**.

To understand the dependence of the stability of the bean structure on parameters more explicitly, we derived an approximate analytical solution. In this analysis, we use the approximation, $\alpha_c \approx 1$, $\alpha_h \approx 0$, and $\phi \approx 1/2$, for the core, in which DNAs are condensed with the mutant condensin complexes, and $\alpha_\mathrm{c} \approx 0$ for the halo, where the mutant condensin complexes are loaded only rarely. Although it is somewhat crude, we also expand the free energy of the halo in the power series of ϕ and α_h at $r = r_\mathrm{c}$ and neglect higher order terms. Leaving the details of the derivation to sec. S2 in the Supplemental File, we here outline the main results of this analysis.

The chemical potential $\mu_\mathrm{c}^\mathrm{th}$ of the mutant condensin complexes at the swollen-condensed transition has an approximate form

$$\mu_\mathrm{c}^\mathrm{th} \simeq \left(\epsilon_\mathrm{c} - (\epsilon_\mathrm{h} - \mu_\mathrm{h}) - \frac{1}{2}\chi + 2\right) + \delta\mu_\mathrm{c}^\mathrm{ela}, \tag{28}$$

where $\delta\mu_\mathrm{c}^\mathrm{ela}$ is the contribution of the entanglement free energy in the core and is a function only of $G_0 b_0^3/(\rho \phi_0^{\frac{1}{3}} k_\mathrm{B} T)$ (and $\epsilon_\mathrm{h} - \mu_\mathrm{h}$), see eq. (S47) and Fig. S5 in the Supplemental File. The maximum chemical potential of the mutant condensin complexes of the bean structure

has an approximate form

$$\mu_{\mathrm{c}}^{\max} \simeq \left(\epsilon_{\mathrm{c}} - (\epsilon_{\mathrm{h}} - \mu_{\mathrm{h}}) - \frac{1}{2}\chi + 2\right) - \frac{1}{(c_0\phi_{\mathrm{m}})^{\frac{1}{3}}}\log\frac{e^4}{(c_0\phi_{\mathrm{m}})^{\frac{1}{3}}} - \frac{c_1}{\rho}\frac{G_0 b_0^3}{\phi_0^{\frac{1}{3}} k_{\mathrm{B}}T}, \tag{29}$$

where c_0 (≃1.5) and c_1 (≃0.8) are numerical constants of order unity. Eqs. (28) and (29) were derived in the asymptotic limit of large negative values of $\epsilon_{\mathrm{h}} - \mu_{\mathrm{h}}$, although it is somewhat crude for the parameters used for our numerical calculations, see sec. S2 in the Supplemental File. The first term of eq. (29) is the contribution of the interaction parameter χ, the free energy $\epsilon_{\mathrm{h}} - \mu_{\mathrm{h}}$ gained by assembling nucleosomes, and the free energy ϵ_{c} gained by loading condensin complexes. The two chemical potentials, $\mu_{\mathrm{c}}^{\max}$ and $\mu_{\mathrm{c}}^{\mathrm{th}}$, have the same dependence on χ, $\epsilon_{\mathrm{h}} - \mu_{\mathrm{h}}$, ϵ_{c}, implying that these parameters do not contribute to the stability of the bean structure, relative to the all-swollen state, at least, in the leading order contributions, see the first terms of eqs. (28) and (29). The second and third terms of eq. (29) are the contributions of the elastic free energy of the DNA loops in the halo and that due to the entanglement in the core to $\mu_{\mathrm{c}}^{\max}$, respectively. These elastic free energies contribute to suppressing the formation of the halo, see the negative sign in the second and third terms of eq. (29). The rescaled shear modulus $G_0 b_0^3/(\phi_0^{\frac{1}{3}} k_{\mathrm{B}}T)$ is smaller than $\frac{b_0^3}{b^3} \approx 8$, while the ratio $\rho \simeq 22$ is a relatively large value, implying that the entanglement free energy in the core is compensated by condensin complexes that protect DNAs from nucleosome assembly, see eq. (11) and Table 1 (but it can still contribute significantly to the destabilization of the all-swollen state via $\delta\mu_{\mathrm{c}}^{\mathrm{ela}}$, see Fig. S1**c** in Supplemental File). The free energy due to the excluded volume interaction between nucleosomal DNAs in the halo, the second term of eq. (29), is thus the most significant barrier to the assembly of the bean structure and this barrier decreases with increasing the volume ratio ϕ_{b}.

DISCUSSION

We have constructed a minimal model to provide insights into the formation of bean structures on entangled DNAs. Our model is constructed based on the assumption that DNA units become elastically ineffective because of nucleosome enrichment and looping in the halo, whereas condensin-condensin interactions make nucleosome-sparse, entangled DNAs elastically effective in the core. Although the conversion of DNA elasticity due to the assembly and disassembly of nucleosomes was taken into account in previous theoretical studies on the brushes of nucleosomal DNAs (Yamamoto and Schiessel, 2016, Yamamoto and Schiessel, 2017**a** and **b**, Leidescher et al., 2020), its role in mitotic chromosome assembly has not been addressed. Our current theory predicts that the loop extrusion-independent

DNA looping is driven by the accumulation of nucleosomes in the halo, where it reels DNAs out from a compacted entangled DNA network in the core. The formation of the halo increases the elastic free energy of entangled DNAs in the core and also increases the free energy due to the excluded volume interaction between DNAs in the halo. We predict that condensin complexes protect DNAs in the core from nucleosomal assembly to compensate the elastic free energy cost of entangled DNAs in the core and entrap the bean structure in the local free energy minimum. The free energy cost due to the excluded volume interaction between DNAs in the halo still remains and thus the bean structure is not the global free energy minimum (see also the discussion below). Despite its simplicity, our theory captures the essential features of the bean structure observed experimentally (Kinoshita et al., 2022), such as the profile of DNA volume fraction and the concentration dependence of bean radius.

Our theory also predicts that the bean structure is a local, but perhaps not the global, free energy minimum. There are three possible reasons why the bean structure was observed in the experiment (Kinoshita et al., 2022): First, the bean structure is a local minimum and thus is kinetically trapped if one decreases the concentration of the mutant condensin complexes from entangled chromosomes in the all-condensed state. In the experiments using mouse sperm nuclei as a substrate in *Xenopus* egg extracts, the loading of condensin complexes precedes the full assembly of nucleosomes (Shintomi et al., 2017), suggesting that the kinetic trapping of the bean structure is a possible scenario. Second, there is an additional mechanism to stabilize the bean structure. In our theory, we treated DNA as a uniform polymer. However, the energy ϵ_{h} gained by assembling nucleosomes is probably different at different regions of chromosomes. If chromosomes act as block copolymers composed of two (or more) different blocks, where the energy gain ϵ_{h} of one block is different from the other, it can be the additional mechanism to stabilize the bean structure. Assuming chromosomes as multi-block copolymers may also explain why the halo is composed of many loops. Third, we may have underestimated the volume ratio ϕ_{m} and/or the rescaled shear modulus $G_0 b_0^3/(\rho\phi_0^{1/3}k_{\mathrm{B}}T)$ due to the entanglement. Experimentally testing these possibilities would clarify how the nucleosomal assembly and the condensin-condensin interactions act to assemble the bean structure and mitotic chromosomes.

If the bean structure is the global free energy minimum, due to the second or third possibility shown in the previous paragraph, this structure would be observed at the chemical potential $\mu_{\mathrm{c}}^{\mathrm{th}}$ of the mutant condensin complexes at the swollen-condensed phase transition, where the swollen and condensed states are both stable. Experimentally, the fluorescence from the mutant condensin complexes was not uniform at the core of the bean: the mutant condensin complexes are condensed more at the periphery than the interior (Kinoshita et al., 2022).

This may imply the coexistence of the swollen and condensed phases in the core, akin to polymer gels at the volume phase transition. Treating the two-phase coexistence in the core is beyond the scope of this paper, because new elements involved in the coexistence, such as the mechanical coupling of the two coexisting phases (Sekimoto, 1993, Tomari and Doi, 1995) and the distribution of DNA units between these phases by sliding through effective crosslinks, make the theory more complex. Moreover, an additional stabilizing mechanism, such as assuming chromosomes as block copolymers, is necessary. Future studies are necessary to treat these elements. Assuming chromosomes as block copolymers implies that the assembly of the bean structure is already tailored into the base sequences of chromosomes. Our present theory forms a basis of a theory that considers these elements and should be constructed before making rather arbitrary assumptions.

In our current theory, we assume that multivalent interactions of DNA-bound condensin complexes contribute to mitotic chromatin compaction, similar to the previous and recent models (Sakai et al., 2018, Forte et al., 2022). On the other hand, it has been proposed that bivalent DNA-cohesin-DNA bridging interaction drives the condensation of DNA-cohesin complexes (Ryu et al., 2021), somewhat analogous to the Semenov-Rubinstein theory of associative polymers in a solution (Semenov and Rubinstein, 1998). Because the postulated condensin-condensin interactions are under the control of SMC ATPase cycle (Kinoshita et al., 2022), such non-equilibrium switching of the condensin-condensin interactions would only decrease its magnitude if this interaction were multivalent (see eq. (18)). For this reason, we considered the cross-talk between condensin and nucleosomes to explain the formation of the halo in the current study. However, if the condensin-condensin interactions were bivalent, as proposed for cohesin by Ryu et al (2021), the non-equilibrium switching would affect the chromosome structure more prominently. In this case, an alternative mechanism that explains the assembly of the halo might exist.

To extend our theory to the mechanism of mitotic chromosome assembly, it is necessary to consider the loop extrusion activity of condensin complexes and the strand-passing activity of topo II. If condensin complexes localized to the core start to extrude loops, they will generate tension of the DNAs entangled in the core so that the DNAs in the halo are reeled into the core (Yamamoto and Schiessel, 2022). The magnitude of the interaction between wild-type condensin complexes may be smaller than the magnitude of the interaction between mutant condensin complexes because CAP-G subunits counteract with CAP-D2 subunits (Kinoshita et al., 2015). Consistent with this prediction, the wild-type condensin complexes form the so-called ‘entangled mass’, in which the halo and core are not structurally differentiated, under the same condition (Kinoshita et al, 2022). An extension of our theory

by taking into account the loop extrusion activity may account for the difference in chromosome structures assembled by wild-type and different mutant condensin complexes. Topo II disentangles and individualizes chromosomes through its strand-passing activity (Pommier et al., 2016). The disentanglement of polymers results from the thermal motion of polymers that slip out of the effective crosslinks from the polymer ends – the reptation dynamics (Doi and Edwards, 1986, Likhtman and McLeish, 2002). The strand-passing activity of topo II can be viewed as transiently creating `ends' in the middle of DNAs and thus can be treated by taking into account the reptation dynamics in an extension of our theory. The individualization of chromosomes changes the geometry of the system (from a concentrated or semi-dilute regime to a dilute regime) and a separate treatment is necessary. Nevertheless, the elastic control of chromosomes via the crosstalk between condensin complexes and nucleosomes is an emerging concept that not only enriches our understanding of the mechanism of mitotic chromosome assembly but also will be useful for studying the mechanics of mitotic chromosomes, such as the action of mechanical forces to separate two sister chromatids.

Data availability

The Mathematica file "beanmodelVer37(revisedformalism).nb" used for the numerical calculations is available in figshare with the identifier (https://doi.org/10.6084/m9.figshare.21517056).

Conflict of interest statement

The authors declare no conflict of interest.

Funding

This work was supported by Grant-in-Aid for Scientific Research/KAKENHI (#20H05934, #21H00241, and #21K03479 [to TY], #19K06499 [to KK], #18H05276 and #20H0593 [to TH]).

References

Alexander, S. 1977. Adsorption of chain molecules with a polar head a scaling description. *J. Phys. (Paris)* 38: 983-987.

Alipour, E., and J. Marko. 2012. Self-organization of domain structures by DNA-loop-extruding enzymes. *Nucleic Acids Res.* 40: 11202-11212.

Ball, R. C., M. Doi, S. F. Edwards, and M. Warner. 1981. Elasticity of entangled networks.

Polymer. 22: 1010-1018.

Blossey, R. and H. Schiessel. 2011. The dynamics of the nucleosome: thermal effects, external forces, and ATP. *FEBS J.* 278: 3619-3632.

Brackley, C.A., S. Taylor, A. Papantonis, P.R. Cook, and D. Marenduzzo. 2013. Nonspecific bridging-induced attraction drives clustering of DNA binding proteins and genome organization. *Proc. Nat. Acad. Sci. USA.* 110: E3605-E3611.

Brackley, C. A., B. Liebchen, D. Michieletto, F. Mouvet, P. R. Cook, and D. Marenduzzo. 2017. Ephemeral protein binding to DNA shapes stable nuclear bodies and chromatin domains. *Biophys. J.*, 112: 1085-1093.

Bracha, D., E. Karzbrun, G. Shemer, P. A. Pincus, and R. H. Bar-Ziv. 2013. Entropy-driven collective interactions in DNA brushes on a biochip. *Proc. Nat. Acad. Sci. USA*. 110: 4534-4538.

Daoud, M. and J. P. Cotton. 1982. Star shaped polymers: a model for the conformation and its concentration dependence. *J. Phys. (Paris).* 43: 531-538.

de Gennes, P. G. 1980. Conformations of polymers attached to an interface. *Macromolecules.* 13: 1069-1075.

Doi, M. and S. F. Edwards. 1986. The theory of polymer dynamics. Oxford University Press, Oxford, UK.

Edwards. S. F. 1967. The statistical mechanics of polymerized material. *Proc. Phys. Soc.* 92: 9-16.

Flory, P. J., and J. Rehner. 1943. Statistical mechanics of cross-linked polymer networks. *J. Chem. Phys.* 11: 521-526.

Forte, G., L. Boteva, N. Gilbert, P. R. Cook, D. Marenduzzo. 2022. Bridging-mediated compaction of mitotic chromosomes. *bioRxiv*. doi: 10.1101/2022.09.27.509716.

Ganji, M., I. A. Shaltiel,, S. Bisht, E. Kim, A. Kalichava, C. H. Haering, and C. Dekker. 2018. Real-time imaging of DNA loop extrusion by condensin. *Science.* 360: 102-105.

Gibcus, J. K. Samejima, A. Goloborodko, I. Samejima, N. Naumova, J. Nuebler, M. T. Kanemaki, L. Xie, J. R. Paulson, W. C. Earnshaw, L. A. Mirny, and J. Dekker. 2018. A pathway

for mitotic chromosome formation. *Science.* 359: eaao6135.

Goloborodko, A., J. F. Marko, and L. Mirny. 2016a. Chromosome compaction by active loop extrusion. *Biophys. J.* 110: 2162-2168.

Goloborodko, A., M. V. Imakaev, J. F. Marko, L. Mirny. 2016b. Compaction and segregation of sister chromatids via active loop extrusion. *elife*. 5:e14864.

Hassler, M., I.A. Shaltiel, M. Kschonsak, B. Simon, F. Merkel, L. Thärichen, H.J. Bailey, J. Macošek, S. Bravo, J. Metz, J. Henning, and C.H. Haering. 2019. Structural basis of an asymmetric condensin ATPase cycle. *Mol. Cell.* 74: 1171-1188.

Hirano, T. 2016. Condensin-based chromosome organization from bacteria to vertebrates. *Cell,* 164: 847-857.

Kimura, K., and T. Hirano. 1997. ATP-dependent positive supercoiling of DNA by 13S condensin: A biochemical implication for chromosome condensation. *Cell*. 90:625-634.

Kinoshita, K., T. J. Kobayashi, and T. Hirano. 2015. Balancing acts of two HEAT subunits of condensin I support dynamic assembly of chromosome axes. *Dev. Cell.* 6: 94-106.

Kinoshita, K., Y. Tsubota, S. Tane, Y. Aizawa, R. Sakata, K. Takeuchi, K. Shintomi, T. Nishiyama, and T. Hirano. 2022. A loop extrusion-independent mechanism contributes to condensin I-mediated chromosome shaping. *J. Cell Biol.* 221: e202109016.

Kong, M., E. E. Cutts, D. Pan, F. Beuron, T. Kaliyappan, C. Xue, E. P. Morris, A. Musacchio, A. Vannini, and E. C. Greene. 2020. Human condensin I and II drive extensive ATP-dependent compaction of nucleosome-bound DNA. *Mol. Cell.* 79: 99-114.

Lee, B.G., F. Merkel, M. Allegretti, M. Hassler, C. Cawood, L. Lecomte, F. J. O'Reilly, L.R. Sinn, P. Gutierrez-Escribano, M. Kschonsak, S. Bravo, T. Nakane, J. Rappsilber, L. Aragon, M. Beck, J. Löwe, and C.H. Haering. 2020. Cryo-EM structures of holo condensin reveal a subunit flip-flop mechanism. *Nat. Struct. Mol. Biol.* 27: 743-751.

Leidescher, S., J. RIbisel, S. Ullrich, Y. Feodorova, E. Hildebrand, A. Galitsyna, S. Bultmann, S. Link, K. Thanisch, C. Mulholland, J. Dekker, H. Leonhardt, L. Mirny, and I. Solovei. 2022. Spatial organization of transcribed eukaryotic genes. *Nat. Cell Biol.* 24: 327-339.

Likhtman, A. E. and T. C. B. McLeish. 2002. Quantitative theory for linear dynamics of linear entangled polymers. *Macromolecules*. 35: 6332-6343.

Likhtman, A. E. 2005. Single-chain slip-link model of entangled polymers: Simultaneous description of neutron spin-echo, rheology, and diffusion. *Macromolecules.* 38: 6128-6139.

Marko, J. F., and E. D. Siggia. 1995. Stretching DNA. *Macromolecules.* 28: 8759-8770

Masubuchi, Y. 2021. Elasticity of randomly cross-linked networks in primitive chain network simulations. *Nihon Reoroji Gakkaishi.* 49: 73-78.

Naumova, N., M. Imakaev, G. Fudenberg, Y. Zhan, B. R. Lajoie, L. A. Mirny, and J. Dekker. 2013. Organization of the mitotic chromosome. *Science.* 342: 948-953.

Nguyen, T. T., and B. I. Shklovskii. 2001. Overcharging of a macroion by an oppositely charged polyelectrolyte. *Physica A.* 293: 324-338.

Park, S. Y., R. F. Bruinsma, and W. M. Gelbart. 1999. Spontaneous overcharging of macro-ion complexes. *Europhys. Lett.* 46: 454-460

Pommier, Y., Y. Sun, S.N. Huang, and J. L. Nitiss. 2016. Roles of eukaryotic topoisomerases in transcription, replication, and genomic stability. *Nat. Rev. Mol. Cell Biol.* 17: 703-721.

Rosa, A. and R. Everaers. 2008. Structure and dynamics of interphase chromosomes. *Plos Comp. Biol.* 4: e1000153.

Rubinstein, M. and R. H. Colby. 2003. Polymer physics. Oxford University Press, Oxford, UK.

Ryu, J. K., C. Bouchoux, H. W. Liu, E. Kim, M. Minamino, R. de Groot, A. J. Katan, A. Bonato, D. Marenduzzo, D. Michieletto, F. Uhlmann, and C. Dekker. 2021. Bridging-induced phase separation induced cohesin SMC protein complexes. *Sci. Adv.* 7: eabe5905.

Sakai, Y., A. Mochizuki, K. Kinoshita, T. Hirano, and M. Tachikawa. 2018. Modeling the functions of condensin in chromosome shaping and segregation. *Plos Comp. Biol.* 14: e1006152.

Sekimoto, K. 1993. Temperature hysteresis and morphology of volume phase transition of gels. *Phys. Rev. Lett.* 70: 4154-4157.

Semenov, A. N. and M. Rubinstein. 1998. Thermoreversible gelation in solutions of associative polymers. 1. Statics. Macromolecules. 31: 1373-1385.

Shintomi, K., T. S. Takahashi, and T. Hirano. 2015. Reconstitution of mitotic chromatids with a minimum set of purified factors. *Nat. Cell Biol.*, 17: 1014-1023.

Shintomi, K., F. Inoue, H. Watanabe, K. Ohsumi, M. Ohsugi, and T. Hirano. 2017. Mitotic chromosome assembly despite nucleosome depletion in Xenopus egg extracts. *Science.* 356: 1284-1287.

Shintomi, K., and T. Hirano. 2021. Guiding functions of the C-terminal domain of topoisomerase IIa advance mitotic chromosome assembly. *Nat. Comm.* 12: 2917.

Socol, M., R. Wang, D. Jost, P. Carrivain, C. Vaillant, E. L. Cam, V. Dahirel, C. Normand, K. Bystricky, J. M. Victor, O. Gadal, and A. Bancaud. 2019. Rouse model with transient intramolecular contacts on a time scale of seconds recapitulates folding and fluctuation of yeast chromosomes. *Nucleic Acids Res.* 47: 6195-6207.

Terakawa, T., S. Bisht, J. M. Eeftens, C. Dekker, C. H. Haering, and E. C. Greene. 2017. The condensin complex is a mechanochemical motor that translocates along DNA. *Science*. 358: 672-676.

Tomari, T., and M. Doi. 1995. Hysteresis and incubation in the dynamics of volume transition of spherical gels. *Macromolecules*. 28: 8334-8343.

Uneyama, T., and Y. Masubuchi. 2012. Multi-chain slip-spring model for entangled polymer dynamics. *J. Chem. Phys.* 137: 154902.

Yamamoto, T., and H. Schiessel. 2016. Transcription driven phase separation in chromatin brush. *Langmuir.* 32. 3036-3044.

Yamamoto, T., and H. Schiessel. 2017a. Transcription dynamics stabilizes nucleus-like layer structure in chromatin brush. *Soft Matter.* 13. 5307-5316.

Yamamoto, T., and H. Schiessel. 2017b. Chromatin gels are auxetic due to cooperative nucleosome assembly and disassembly dynamics. *Europhys. Lett.* 118: 28003.

Yamamoto, T., and H. Schiessel. 2022. Loop extrusion driven volume phase transition of entangled chromosomes. *Biophys. J.* 121: 2742–2750.

Yamamoto, T., J. Campbell, S. Panyukov, and M. Rubinstein. 2022. Scaling theory of swelling and deswelling of polymer networks. *Macromolecules.* 55: 3588-3601.

Yokota, H., and M. Tachikawa. 2022. Evaluation of loop formation dynamics in a chromatin fiber during chromosome condensation. *Prog. Theo. Exp. Phys.* 2022: 053J01.

FIGURE LEGENDS

Figure 1 Polymorphism of chromatin structures observed in *Xenopus* egg extracts. Shown above are chromatin structures observed under different conditions in *Xenopus* egg extracts. Shown below are more detailed structures with mutant condensin I complexes deficient in loop extrusion (orange circles) and DNA units (green circles). **a.** Abnormal chromosome-like structures observed in a condensin-depleted extract (Δcond extract) that is supplemented with a condensin I mutant. **b.** A 'cloud'-like structure observed in a condensin/topo II-depleted extract (Δcond Δtopo II extract). **c.** A 'bean' structure observed in a condensin/topo II-depleted extract (Δcond Δtopo II extract) that is supplemented with the condensin I mutant. Under the conditions of **b** and **c**, entangled DNAs behave as a polymer network.

Figure 2 Elastically effective and ineffective chains in an entangled DNA network. a. Three possible structures formed by entangled DNAs: the all-swollen state (left), the bean structure (middle), and the all-condensed state (right). **b**. DNA chains connected to the network at two points via effective crosslinks due to DNA entanglements (magenta) respond to the deformation of the network and thus are elastically effective (indicated by the black broken lines). DNA units wrapped around histones (yellow circles) do not respond to such network deformation and thus are elastically ineffective (indicated by the cyan broken line). **c**. The DNA loops in the halo do not contribute to the elastic free energy, thereby being elastically ineffective.

Figure 3 Model of the bean structure. The bean is composed of the core and the halo. DNA and the mutant condensin complexes, lack of loop extrusion activity, are condensed in the core and DNA loops are packed and extended in the halo. The core and the halo are modeled as an entangled DNA network and a brush of DNA loops. A fraction N_{c}/N of DNA units is distributed in the core and the other DNA units are distributed in the halo. The bean is characterized by the DNA volume fraction ϕ, the occupancies, α_c *and* α_h, of DNA by the mutant condensin complexes and nucleosomes.

Figure 4 Affine deformation. In the relaxed (reference) state, the radius of the core is r_{c0} and the average distance between the two effective crosslinks that connect a DNA chain composed of N_{e0} is R_0. If the core is swollen or deswollen so that the radius becomes $\lambda_{\mathrm{s}} r_{\mathrm{c0}}$, the radius of the core changes to $r_{\mathrm{c}}(=\lambda_{\mathrm{s}} r_{\mathrm{c0}})$ and the average distance between the effective crosslinks become $\lambda_{\mathrm{s}} R_0$ (affine deformation). The number of DNA units in the chain between the effective crosslinks becomes N_{e}.

Figure 5 Profiles of DNA volume fraction and occupancies of DNA by the mutant condensin complexes and nucleosomes. The DNA volume fraction (black) and the occupancies, α_{c} and α_{h}, of DNA by the mutant condensin complexes (orange) and nucleosomes (light green). The values of parameters used for the calculation are summarized in Table 1, except for the chemical potential $\mu_{\mathrm{c}} - \epsilon_c$ = - 2.8 of the mutant complexes.

Figure 6 DNA is reeled into core with increasing the concentration of the mutant condensin complexes. a. The radii of the core r_{c} (red) and the bean r_{b} (blue) are shown as functions of the exponential $\exp(\mu_{\mathrm{c}} - \epsilon_{\mathrm{c}})$, which is proportional to the concentration of the mutant condensin complexes in the exterior solution. The parameters used for the calculation are summarized in Table 1. **b.** The fraction of DNA units in the core is shown as a function of the exponential $\exp(\mu_{\mathrm{c}} - \epsilon_{\mathrm{c}})$.

Figure 7 Free energy vs chemical potential of the mutant condensin complexes. The free energy of the system is shown as a function of the chemical potential of the mutant condensin complexes. The values of the free energy of the bean state, the all-condensed state, and the all-swollen state are shown by the green, cyan, and magenta lines, respectively. The parameters used for the calculation are summarized in Table 1.

Figure 1

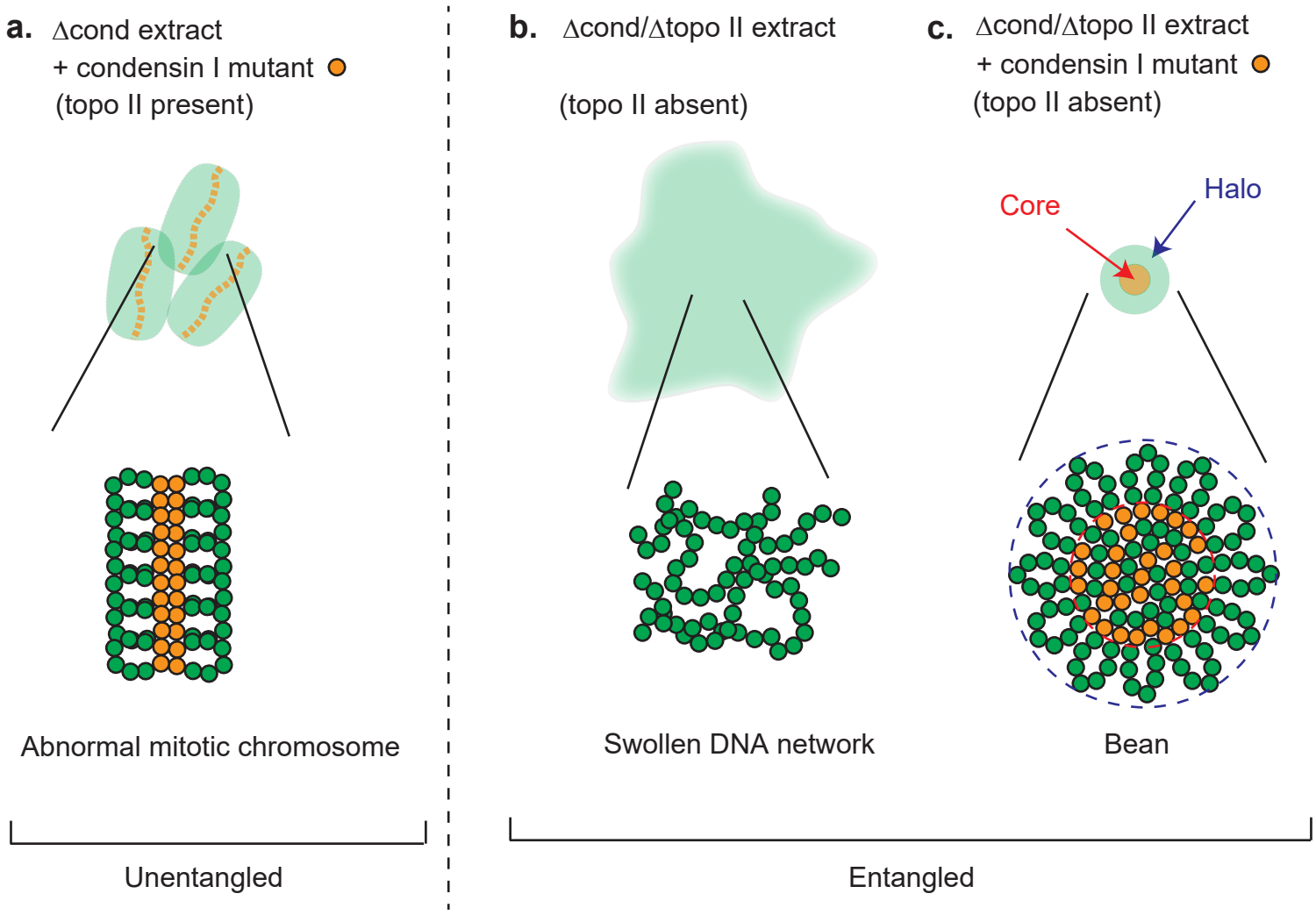
a. Δcond extract
+ condensin I mutant
(topo II present)
Abnormal mitotic chromosome
Unentangled
b. Δcond/Δtopo II extract
(topo II absent)
Swollen DNA network
c. Δcond/Δtopo II extract
+ condensin I mutant
(topo II absent)
Core
Halo
Bean
Entangled

Figure 2

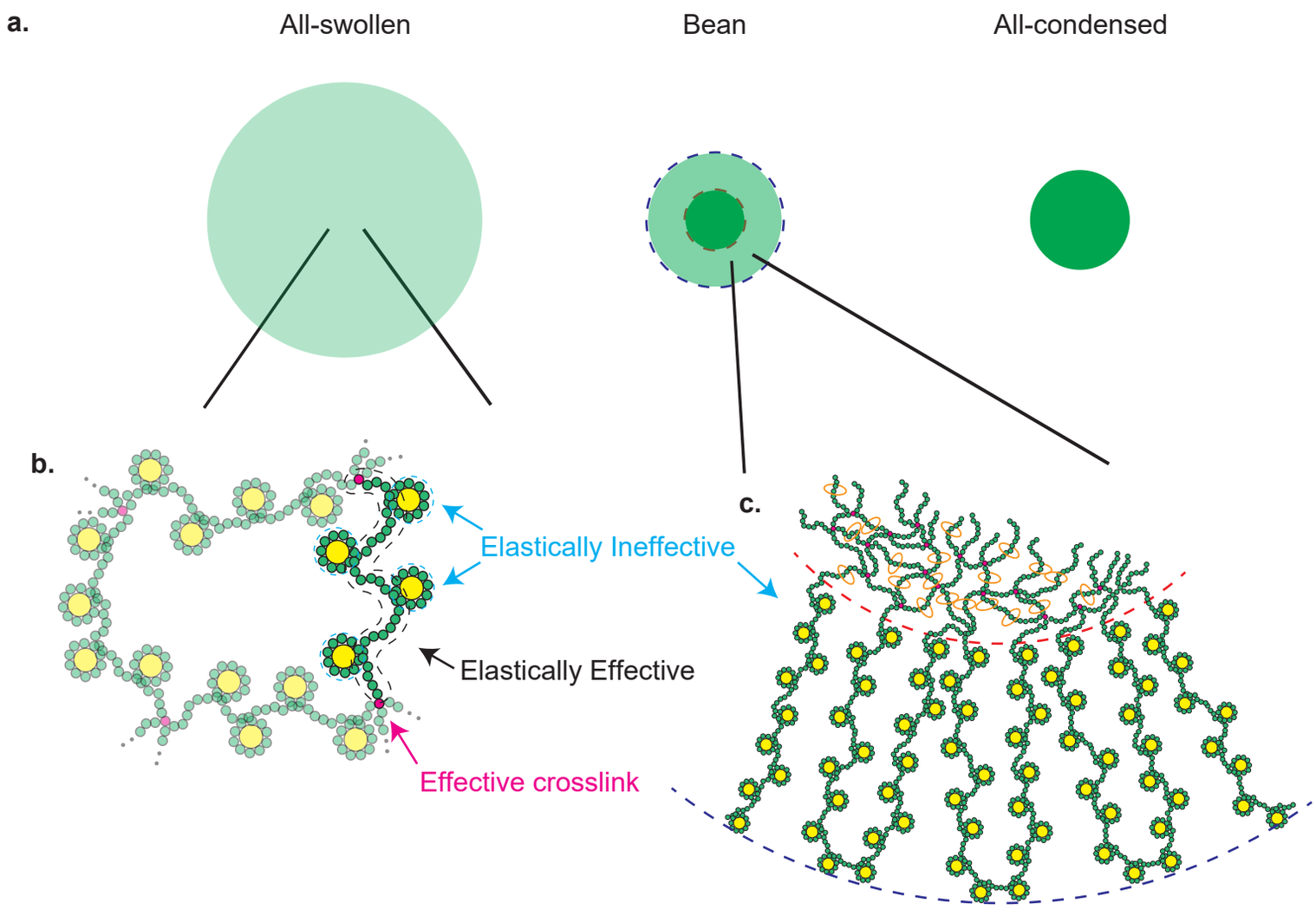
a.
All-swollen
Bean
All-condensed
b.
Elastically Ineffective
Elastically Effective
Effective crosslink
c.

Figure 3

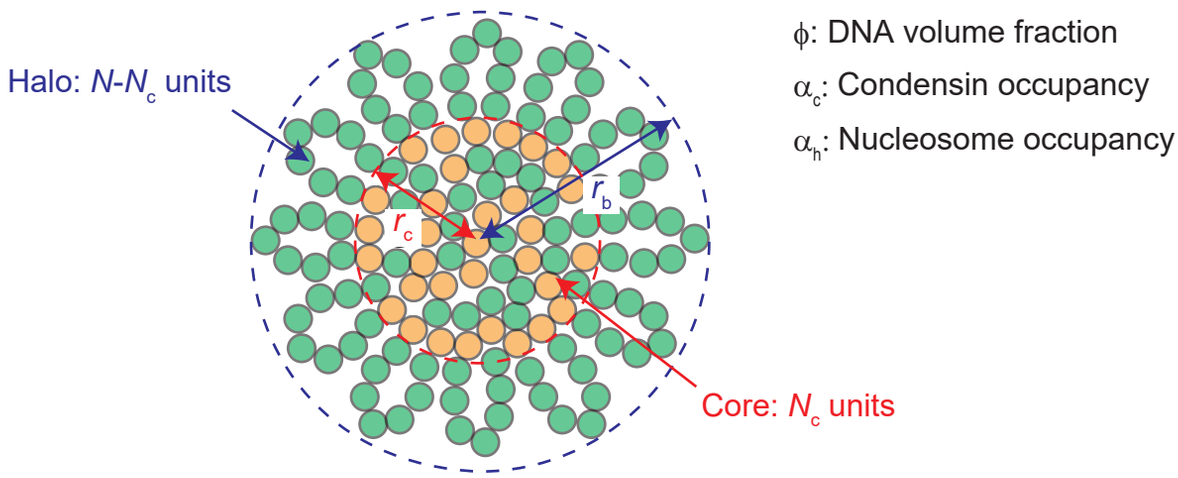
Halo: N-N_c units
r_c
r_b
Core: N_c units
ϕ: DNA volume fraction
α_c: Condensin occupancy
α_h: Nucleosome occupancy

Figure 4

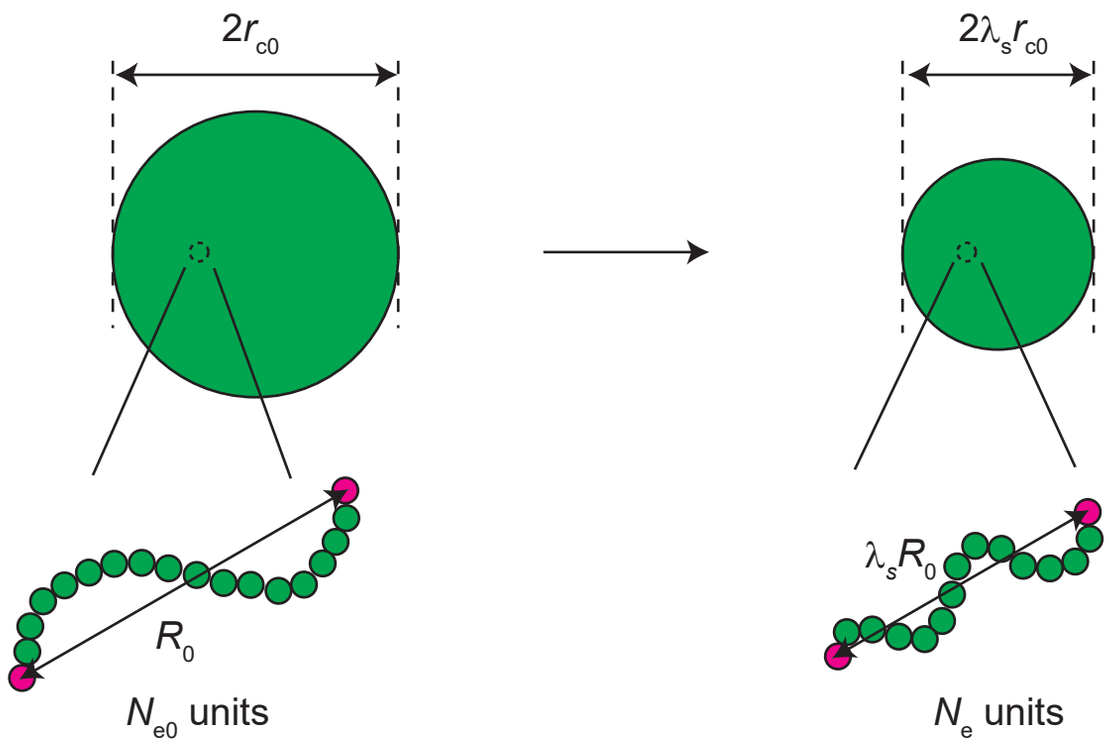

Figure 5

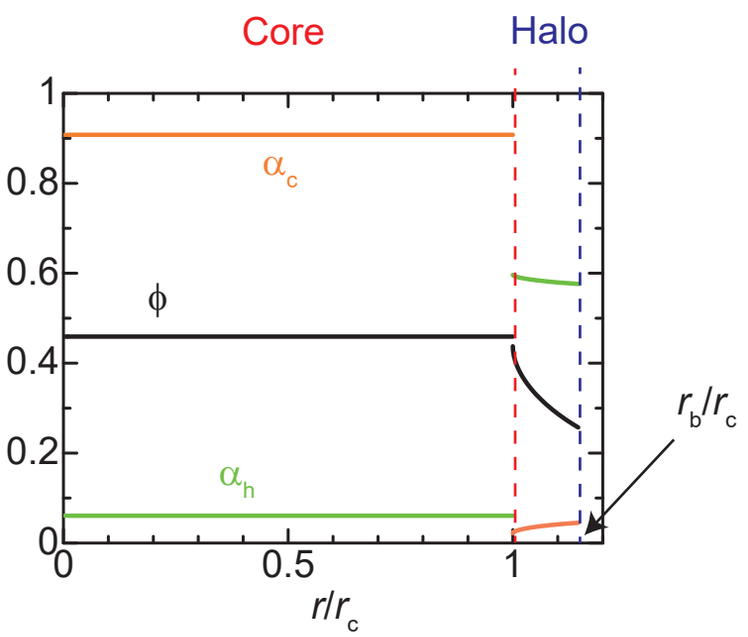

Figure 6

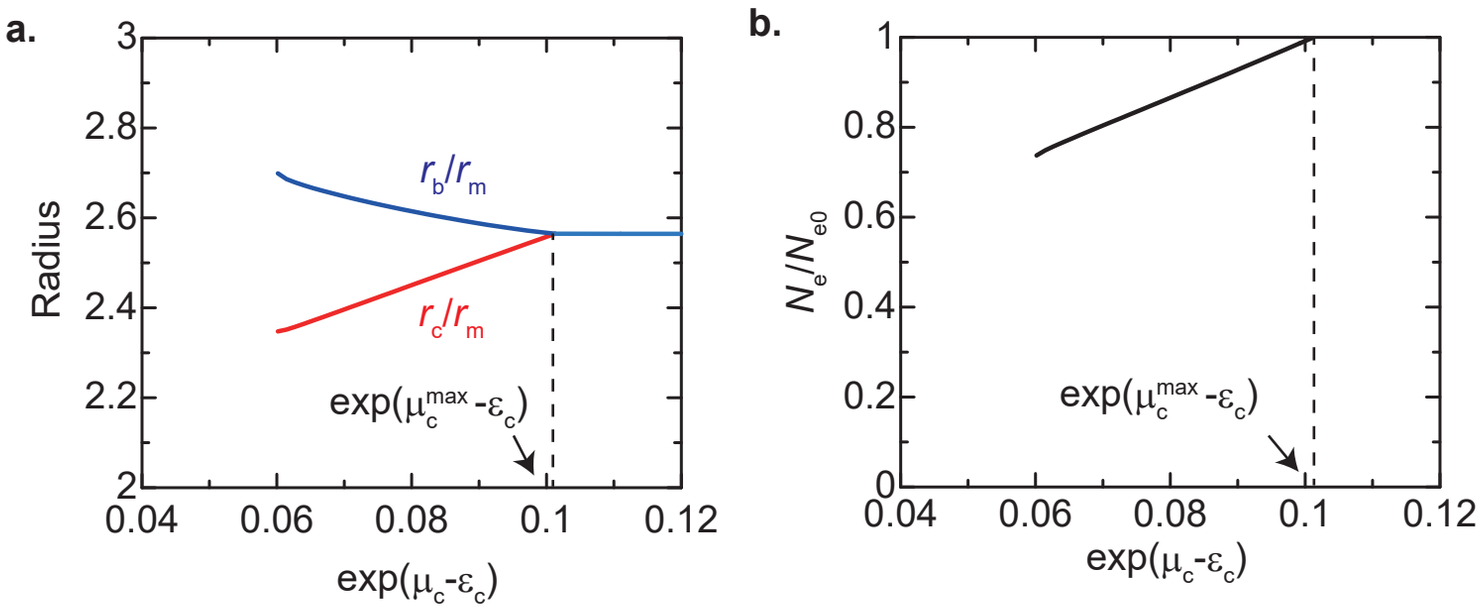
a.
Radius
3
2.8
2.6
2.4
2.2
2
0.04
0.06
0.08
0.1
0.12
r_b/r_m
r_c/r_m
$\exp(\mu_c^{max}-\varepsilon_c)$
$\exp(\mu_c-\varepsilon_c)$
b.
N_e/N_{e0}
1
0.8
0.6
0.4
0.2
0
0.04
0.06
0.08
0.1
0.12
$\exp(\mu_c^{max}-\varepsilon_c)$
$\exp(\mu_c-\varepsilon_c)$

Figure 7

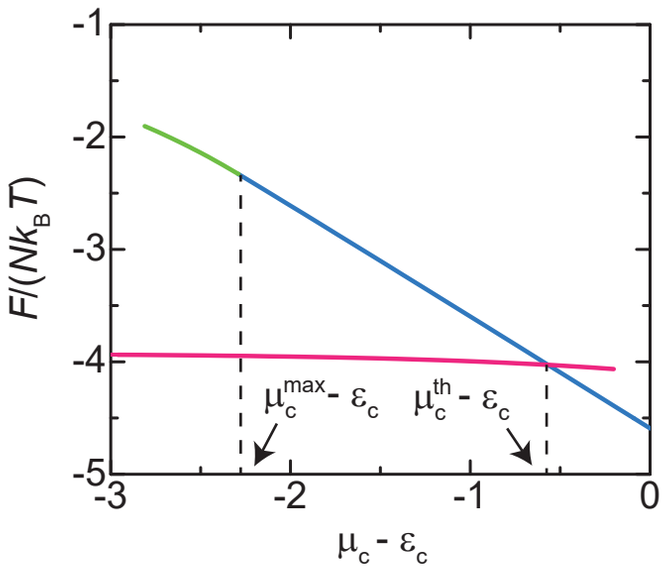
-1
-2
-3
-4
-5
-3
-2
-1
0
$F/(Nk_BT)$
$\mu_c - \varepsilon_c$
$\mu_c^{max} - \varepsilon_c$
$\mu_c^{th} - \varepsilon_c$